Calibration of a helium-cooled infrared spatial radiometer and grating spectrometer

Larry Jacobsen, Steve Sargent, Clair L. Wyatt, Allan J. Steed

Space Dynamics Laboratory
Utah State University, Logan, UT 84321-4140

512-43
171303
P-11

ABSTRACT

Methods used by the Space Dynamics Laboratory of Utah State University (SDL/USU) to calibrate infrared sensors are described, using the Infrared Background Signature Survey (IBSS) spatial radiometer and grating spectrometer as examples. A calibration equation and a radiometric model are given for each sensor to describe their responsivity in terms of individual radiometric parameters. The calibration equation terms include dark offset, linearity, absolute responsivity, and measurement uncertainty, and the radiometric model domains include spatial, spectral, and temporal domains. A portable calibration facility, designed and fabricated by SDL/USU, provided collimated, extended, diffuse scatter, and Jones sources in a single cryogenic dewar. This multi-function calibrator allowed calibration personnel to complete a full calibration of the IBSS infrared radiometer and spectrometer in two 15-day periods. A calibration data system was developed to control and monitor the calibration facility, and to record and analyze sensor data.

1. INTRODUCTION

Electro-optical systems require calibration to verify instrument design, create algorithms necessary for data reduction, and estimate measurement uncertainties. The Space Dynamics Laboratory of Utah State University (SDL/USU) has been calibrating electro-optical instruments since 1970. This paper describes the methods used to calibrate the infrared (IR) sensor of the Infrared Background Signature Survey (IBSS) experiment. The calibration approach is discussed, as well as the data collection and processing methods. Examples of the results obtained by these methods are also provided.

The IBSS experiment is a Strategic Defense Initiative Organization (SDIO)-sponsored shuttleborne program designed to measure ultraviolet (UV), visible, and IR signatures from various sources. The prime contractor for this program is Messerschmitt-Bolkow-Blohm (MBB) of the Federal Republic of Germany. The IBSS hardware includes a cryogenically cooled IR sensor; a UV, visible, and near-infrared spectrograph/imager; a low-light-level television; and additional instrumentation. These primary instruments are located on a shuttle pallet satellite (SPAS) that is based in the shuttle orbiter until deployed for measurement missions.

The IBSS IR sensor consists of a high off-axis rejection telescope, a spatial radiometer, and an Ebert-Fastie grating spectrometer. The radiometer and spectrometer obtain their input energy from the telescope, which focuses energy on the instrument's detector arrays. The fields of view of the 29 radiometer detectors are scanned in object space by an internal scan mirror. The radiometer has a multi-position filter wheel to select a bandpass filter. The 12-detector spectrometer array measures 6 different spectral ranges simultaneously as the diffraction grating is scanned. The sensor operates in the 2.5 - 24 μm infrared spectral region and is housed in a helium-cooled dewar. Both the radiometer and spectrometer have dedicated on-board signal processors that DC restore the chopped detector responses. The IBSS experiment is described in Lange et al.[1]

2. METHODS

2.1. Calibration approach

The approach used by SDL/USU to calibrate radiometric sensors involves generating a specific calibration equation and radiometric model for the sensor being tested. The calibration equation and radiometric model describe the overall responsivity of the sensor in terms of separate radiometric parameters.[2] The calibration equation correlates sensor output to measured flux, while the radiometric model describes the measured flux as a function of the actual flux. The calibration equation for the IBSS radiometer is:

PRECEDING PAGE BLANK NOT FILMED

$$\Phi_m = \frac{1}{\mathfrak{R}_{filt}} L_R(\text{Resp}-\text{DO}_R) \pm \sigma_{filt} \qquad (1)$$

where Φ_m is measured flux, $\mathfrak{R}_{filt}$ is absolute responsivity for a given radiometer filter, L_R is the radiometer linearity correction transfer function, Resp is radiometer response, DO_R is radiometer dark offset, and σ_{filt} is measurement uncertainty for a given radiometer filter.

The calibration equation for the IBSS spectrometer is:

$$\Phi_m(\lambda) = \frac{1}{\mathfrak{R}(\lambda)} L_S[\text{Resp}(\lambda)-\text{DO}_S] \pm \sigma(\lambda) \qquad (2)$$

where $\Phi_m(\lambda)$ is measured spectral flux, $\mathfrak{R}(\lambda)$ is absolute spectral responsivity, L_S is the spectrometer linearity correction transfer function, $\text{Resp}(\lambda)$ is spectrometer response, DO_S is spectrometer dark offset, and $\sigma(\lambda)$ is spectrometer measurement uncertainty.

The radiometric models for the IBSS radiometer and spectrometer characterize their spectral, spatial, and temporal domains. The relative spectral responsivity describes the spectral domain of the radiometer. The grating position, line shape, and spectral leakage analyses describe the spectrometer spectral domain. The field-of-view response maps, detector positions, scatter coefficients, effective fields of view, modulation transfer functions, and scan mirror transfer function describe the spatial domain of the radiometer and spectrometer. The radiometer and spectrometer frequency responses describe the temporal domains of the sensor.

Each term in the calibration equation and each domain in the radiometric model describes a specific radiometric parameter. The goal of the calibration is to characterize each parameter independently of the others. Together, these individually characterized radiometric parameters comprise a complete calibration of a radiometric sensor.

2.2. Portable calibration source (PCS)

Since individual parameters of the sensor calibration equation and radiometric model are best measured with different optical source configurations, SDL/USU personnel designed and fabricated a portable calibration source (PCS) that incorporated four optical functions into a single, cryogenically cooled dewar. These functions included a collimated source; an extended source; a near, small-area (Jones) source; and a diffuse scatter source. This multiple-function calibration source eliminated the sensor warm-up cycles usually required to mate different calibration sources to the sensor, enabling calibration personnel to collect all data required for a full calibration in two 15-working day periods. Wyatt et al.[3] provides a full description of the PCS.

2.3. Calibration data system

SDL/USU personnel developed a computerized calibration data system, consisting of commercially-available and SDL/USU-designed hardware and software, to control the PCS, collect the IBSS telemetry stream, and analyze the resulting calibration data. The system recorded individual "snapshots" of the telemetry stream, automatically inserted a header describing the current configuration of the calibration source, and stored the snapshots on a peripheral optical-media mass-storage device. The data system then retrieved, processed, and organized the snapshots into a calibration data base. This system greatly reduced the time previously required to complete data analysis, allowing calibration personnel to perform all analyses needed to prepare quick-look reports within two weeks of data collection, and to complete the final calibration report in six months.

2.4. Data processing

The IBSS sensor design incorporates a chopper and a signal processor that DC restores the detector responses, giving a complex output. Since this complex output represents a real radiant flux, it must be converted to a real number. Therefore, the calibration described in this paper correlates the amplitude of the complex response to radiant flux. All operations on low-level responses were performed before conversion to amplitude, to avoid misinterpretation of random noise as signal. Throughout this paper, the IBSS response is given in counts as computed by the onboard signal processor, and reported by telemetry.

3. RESULTS

Calibration personnel devised and carried out tests to determine each term in the calibration equations, and to characterize each responsivity domain in the radiometric models. The test results presented in this paper are examples of the data obtained for the IBSS calibration. Where applicable, data from the same detectors are presented. A full description of the IBSS calibration tests and results for all radiometer and spectrometer detectors is presented in the final IBSS calibration report.[4]

3.1. Calibration equation parameters

Calibration personnel measured dark offset, linearity, absolute responsivity, and measurement uncertainty for the IBSS spectrometer and radiometer calibration equations.

Dark offset

To apply the calibration equation, dark offset must first be subtracted from the sensor response. Calibration personnel determined the mean dark offset prior to each calibration test to offset-correct the results of that test. Typical radiometer dark offsets were approximately 8e+3 counts, and typical spectrometer dark offsets were approximately 1e+3 counts.

Linearity

The next step in applying the calibration equation is to linearize the sensor response. The linearity calibration provides a transfer function of actual response to ideal linearized response throughout the sensor dynamic range. Once the sensor response has been linearized, a single coefficient, found during the absolute responsivity calibration, converts linearized response to measured flux. By analyzing linearity independently of the absolute responsivity and other radiometric parameters, calibration personnel can more easily identify errors in the absolute calibration due to sensor spectral leaks and source uncertainties. In addition, since the linearity function covers the entire dynamic range, the absolute (extended) source need not cover the sensor dynamic range in the absolute responsivity calibration.

The ideal source for a linearity calibration provides a wide range of flux without changing the spectral, spatial, or temporal characteristics of the flux. The SDL/USU calibrator offers two sources for the linearity calibration: the Jones source and the collimator. Both sources give fluxes proportional to their aperture areas, but only the smallest collimated apertures fit entirely within the fields of view of the small radiometer detectors; therefore, the Jones source was chosen for the radiometer linearity calibration. Because the Jones source failed to give adequate signal over the spectrometer dynamic range, the collimator was used for the spectrometer linearity calibration. Calibration personnel varied the input flux in known ratios with the set of calibrator precision apertures, and used multiple source temperatures to cover the dynamic range of both sensors.

The radiometer responses to each input flux were offset corrected with dark responses, plotted versus relative flux, and fit to a piecewise, polynomial linearity-correction function. Fig. 1 shows the results of the linearity calibration for radiometer detector 13, which is typical of the radiometer detectors. Linearity uncertainties, computed as the standard deviation of the curve-fit residuals, were less than 2.5% for most detectors. Similar analyses were performed for the spectrometer detectors, which also showed linearity uncertainties of a few percent.
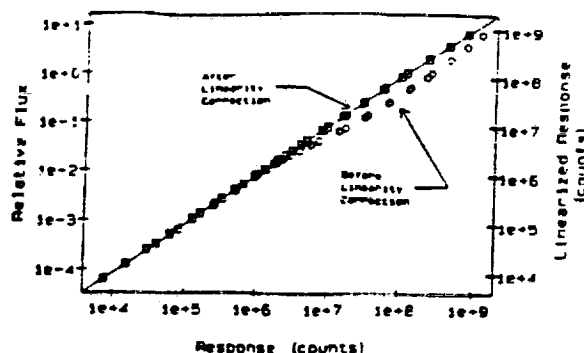
Fig. 1. Radiometer detector 13 linearity calibration.

Absolute responsivity

The absolute responsivity coefficient converts the offset-corrected and linearized sensor response to measured flux. The IBSS spectrometer absolute calibration is presented to illustrate the method used to determine the absolute responsivity coefficient.

The preferred source for the absolute calibration is the extended source because its flux is subject only to temperature and emissivity uncertainties. However, since the extended source has a limited temperature range, other sources, such as the Jones source, can be used to augment the extended source data at short wavelengths. Both the extended and Jones sources were used for the IBSS spectrometer absolute responsivity calibration.

Responses to a number of known fluxes were curve-fit at each wavelength by:

$$\Phi_c(\lambda) = \frac{1}{\Re(\lambda)} \left[Resp_L(\lambda) \right] \tag{3}$$

where $\Phi_c(\lambda)$ = computed spectral radiance in W cm^{-2} sr^{-1} μm^{-1}, $\Re(\lambda)$ = absolute spectral responsivity in counts/W cm^{-2} sr^{-1} μm^{-1}, and $Resp_L(\lambda)$ = offset-corrected and linearized response in counts.

The offset-corrected and linearized responses were curve-fit to equation 3 at each wavelength to give the absolute spectral responsivity. Fig. 2 shows the results of the absolute calibration for detector 5. Curve-fit uncertainties are also shown in this figure. As described in equation 3, the absolute spectral responsivity is given in radiance with units of counts/W cm^{-2} sr^{-1} μm^{-1}. Another useful parameter is the irradiance spectral responsivity, which is the absolute responsivity in flux density with units of counts/W cm^{-2} μm^{-1}. This irradiance responsivity was found by dividing the spectral radiance responsivity by the effective field of view, a parameter discussed in the spatial domain characterization section of this paper.
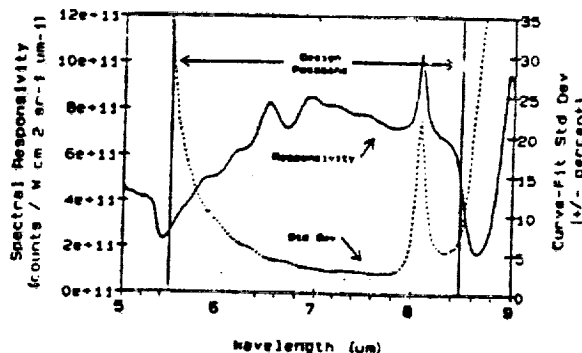

Fig. 2. Spectrometer detector 5 absolute spectral responsivity calibration.

The radiometer absolute calibration was similar, except that the source flux was multiplied by the radiometer relative spectral responsivity, discussed in the spectral domain characterization section of this paper, and integrated over the spectral passband to give a non-spectral absolute responsivity. This analysis was repeated for each detector-filter combination. Curve-fit uncertainties were good, and no spectral errors were observed.

Measurement uncertainties

The calibration equation includes an estimate of the sensor's measurement uncertainty. This estimate consists of the sensor precision and the calibration accuracy. Precision is the reproducibility or consistency of individual measurements. Accuracy is the correlation of the sensor's calibrated response to the true radiometric value. Sensor precision is determined from dark noise, uncertainty of dark offset, signal-to-noise ratio, and long-term repeatability. The total calibration accuracy is given by the root-sum-square combination of the uncertainties from the linearity calibration, absolute responsivity calibration, extended source emissivity, and extended source temperature. The total measurement uncertainty is then determined by the root-sum-square combination of the total sensor precision and total calibration accuracy.

Dark noise is the precision of individual measurements at the minimum detectable signal level. To characterize the dark noise of the IBSS radiometer and spectrometer, calibration personnel collected telemetry data with the IBSS filter wheel in the closed position and used Fourier techniques to compute dark noise spectra. These spectra were then integrated over the noise bandwidth to compute total rms dark noise. These spectra contained noise from the 50-Hz (European) power distribution system, which accounted for about one-half of the total rms noise. It was assumed that this noise will not be present during the deployment of IBSS, and was therefore omitted from the integrations for the total rms dark noise. Typical radiometer dark noise was 3e+3 rms counts and typical spectrometer dark noise was 1e+4 rms counts. The spectrometer dark noise was independent of grating position.

Uncertainty from the long-term drift of dark offset also degrades sensor precision at the bottom of the dynamic range. Calibration personnel recorded dark offsets of the IBSS radiometer and spectrometer each day throughout the data-collection period to measure the dark offset long-term drift. Fig. 3 shows the range of the daily means of the dark offsets for each radiometer detector. Although most calibration results are reported as the amplitude of the complex response, dark offset is presented as a complex number because offset correction of the signal responses must be performed before conversion to amplitude. The ranges shown indicate the uncertainty due to long-term drift of the dark offset.
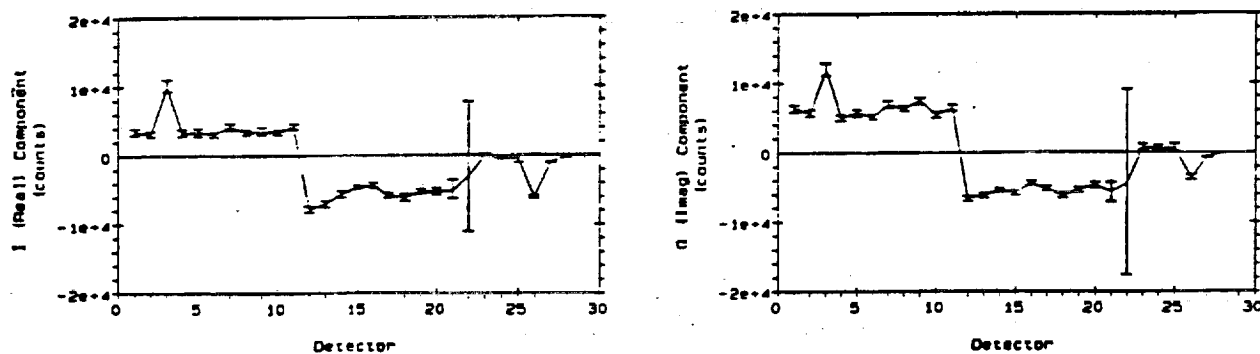

Fig. 3. Dark offsets for all radiometer detectors.

Dark noise and dark offset uncertainty only determine the precision at the bottom of a sensor's dynamic range. At higher flux levels, other noise sources, such as photon noise and digitization noise, must also be considered. The signal-to-noise ratio (SNR) and sensor long-term repeatability provide an indication of precision throughout the entire dynamic range. The total sensor precision can be determined from the SNR and the long-term repeatability, as follows:

$$\sigma_{\text{Precision}} = \sqrt{\frac{1}{\text{SNR}^2} + \sigma_{\text{Rep}}^2} \qquad (4)$$

where $\sigma_{\text{Precision}}$ = total sensor precision, SNR = signal-to-noise ratio, and σ_{Rep} = long-term repeatability.

The spectrometer SNR was characterized by recording the spectrometer's response to collimated sources of various sizes and temperatures. The resulting signals were offset corrected, and the noise for each snapshot was corrected to remove the 50-Hz components. Fig. 4 presents the SNR for one spectrometer detector. As expected, the SNR increased with increasing response. Similar analyses were performed for all other spectrometer and radiometer detectors.
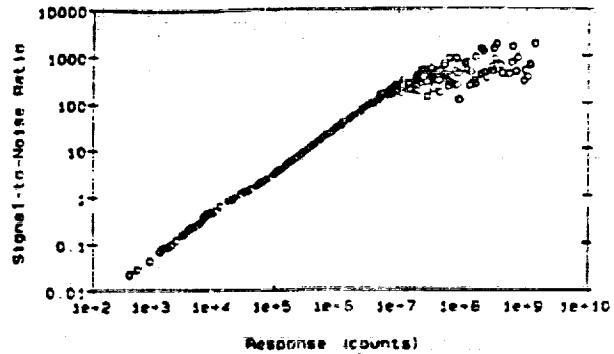
Fig. 4. SNR throughout the dynamic range for detector 5.

To measure the sensor's long-term repeatability, calibration personnel recorded the sensor's response to both the IBSS internal source and the calibrator Jones source daily throughout the calibration period. It was necessary to obtain a comparison between the sensor's response to both sources to evaluate the stability of the IBSS internal source, which is ultimately used to verify the sensor's stability. The standard deviations of the daily internal source and Jones source responses, given as percentages of the overall means, showed that the response to the IBSS internal source was repeatable within ±10 to ±30% for the radiometer detectors, and ±5 to ±17% for the spectrometer detectors. The response to the calibrator Jones source was repeatable within ±5 to ±8% for the radiometer detectors, and ±1 to ±5% for the spectrometer detectors. The Jones source repeatability, depending on the detector, was up to a factor of 4 times better than the internal source repeatability. This indicates that the IBSS internal source itself, rather than the sensor, limited the repeatability of the internal source response.

Fig. 5 presents the total calibration accuracy for all radiometer detectors with one radiometer filter. Analyses for all filter-detector combinations showed typical accuracies of ±5 to ±10%. Fig. 6 presents the total calibration accuracy for spectrometer detector 5. The peak at 8μm is due to a spectral leak, discussed in the spectral domain characterization section of this paper. Typical total calibration accuracies were ±5 to ±12% for the spectrometer detectors.
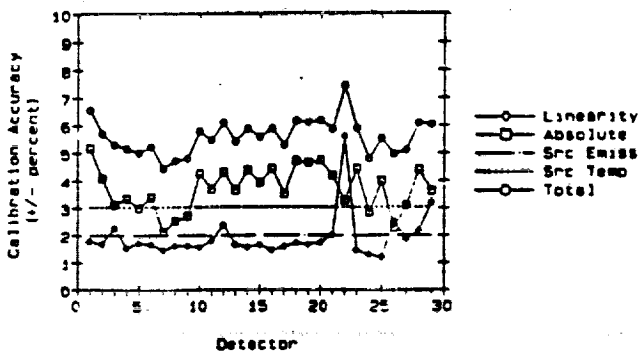

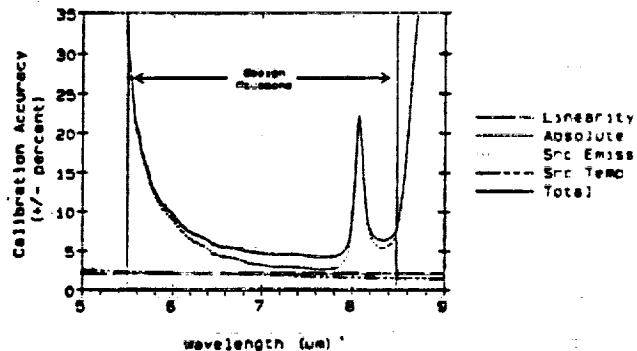Fig. 5. Calibration accuracy estimates for radiometer filter 0 and all detectors.

Fig. 6. Calibration accuracy estimate for spectrometer detector 5.

3.2. Radiometric Model Parameters

Spectral domain characterization

The radiometer's radiometric model includes the relative spectral responsivity, which is the peak-normalized responsivity as a function of the wavelength of the measured radiation. This parameter is used to calculate the effective flux for the absolute calibration and to interpret on-orbit data. Calibration personnel determined the relative spectral responsivity of the IBSS radiometer with each IBSS filter, using an externally chopped blackbody, grating monochromator, and calibrator Jones source. The IBSS internal chopper was turned off, the onboard signal processor was bypassed, and the output was fed into an external lock-in amplifier. The DC-restored output of the lock-in amplifier was normalized with a spectrally flat external reference detector to calculate the spectral responsivity. The spectral responsivity was then normalized to its own peak. Fig. 7 gives the radiometer relative spectral responsivities for each of the IBSS filters.

The spectrometer's radiometric model includes grating position transfer functions, line shape characterization, and spectral leakage analysis. To determine the IBSS spectrometer grating position transfer functions, calibration personnel illuminated the spectrometer with an external monochromator through the Jones source at approximately ten different wavelengths in each grating order. These data were then fit to linear transfer functions. Fig. 8 presents the grating position calibration for each grating order. The end points of each line represent the passband for that grating order. The grating position calibration uncertainties were approximately equal to the design spectral resolution, given by $\Delta\lambda = \lambda/300$ (λ = wavelength).

The line shape calibration evaluates the spectrometer's spectral resolution by measuring its response to a monochromatic source. To determine the IBSS spectrometer line shape, calibration personnel illuminated the spectrometer with a 3.391-μm helium-neon (HeNe) laser through the Jones source. The center wavelength determined by this calibration agreed with the theoretical center wavelength within the grating position calibration uncertainty. The half-power width agreed with the IBSS specified resolution.
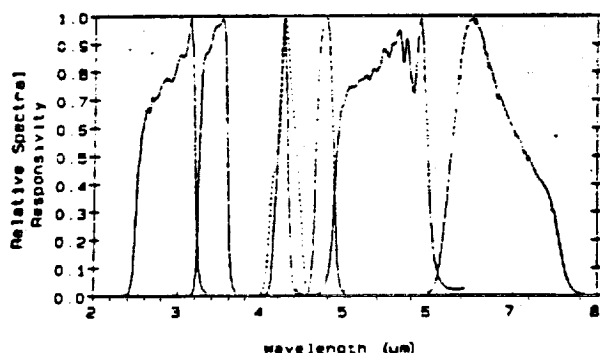

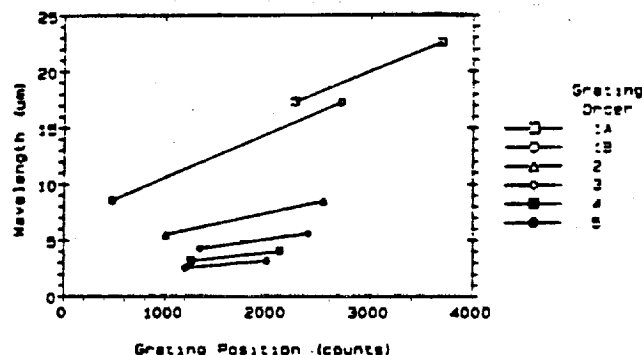Fig. 7. Radiometer relative spectral responsivity.

Fig. 8. Spectrometer grating position calibration.

The spectrometer radiometric model also characterizes the sensor's spectral purity, which is its ability to measure radiation at only the desired wavelength. Since each grating order diffracts energy of a different specific wavelength onto a given detector at a given grating angle, the IBSS spectrometer detectors are covered by order-sorting bandpass filters. The wavelength for higher grating orders are related to that of the first grating order by:

$$\lambda_N = \frac{\lambda_1}{N} \qquad (5)$$

where λ_N = wavelength for order N in μm, λ_1 = wavelength for order 1 in μm, and N = the grating order (1, 2, 3, ...).

The order-sorting filters that cover the IBSS spectrometer detectors are designed to select radiation from only the desired spectral order. However, at certain grating angles, some order-sorting filters also pass radiation of an undesired spectral order. This results in the spectrometer detector simultaneously responding to radiation from more than one wavelength for a given grating angle. Since radiation is "leaking" to the detector from an undesired wavelength, it is said to be the result of a "spectral leak."

To identify spectral leaks, calibration personnel compared the spectrometer's relative spectral responsivities measured using blackbody sources at different temperatures. Ideally the relative spectral responsivity measurement is independent of source temperature. But for grating positions with long-wavelength leaks, a low-temperature source gives an erroneously high relative spectral responsivity. This is because low-temperature sources have proportionately more energy at long wavelengths, which make the long-wavelength leaks more significant. Similarly, for grating positions with short-wavelength leaks, a high-temperature source shows an erroneously high relative spectral responsivity.

Fig. 9 shows the superimposed spectrometer detector 5 relative spectral responsivities measured using Jones and extended source temperatures from 185 to 1269 Kelvin. Three spectral leaks are identified. Calibration personnel quantified these leaks by computing the ratio of the absolute responsivity at the leaked wavelength to the absolute responsivity at the unleaked wavelength. This ratio was 3% for the leak at 5.49 μm, 20% for the leak at 8.08 μm, and 9% for the leak at 8.33 μm. Two additional spectral leaks were characterized in the other four spectral grating orders.
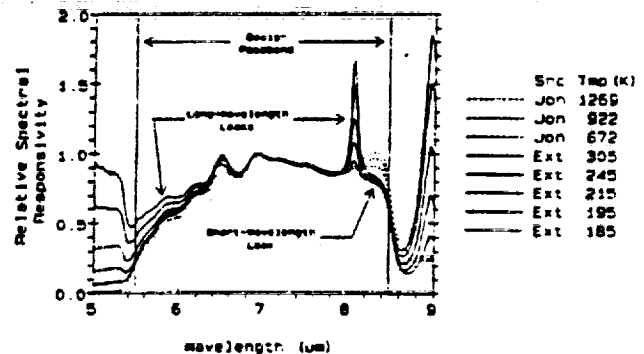

Fig. 9. Spectrometer detector 5 spectral leakage characterization.

Spatial domain characterization

The spatial domain characterization is best illustrated by the IBSS radiometer spatial calibration; therefore, only radiometer data is discussed. Calibration personnel measured the radiometer's spatial responsivity by positioning an 80-μrad collimated source at 0.1 mrad increments over the entire focal plane. The detector responses at each location were offset corrected, linearity corrected, and peak normalized. These data were then analyzed to provide field-of-view response maps, relative detector positions, scatter coefficients, effective fields of view, and modulation transfer functions (MTF). A similar calibration was performed for the spectrometer, with the grating stopped.

Figs. 10 and 11 give field-of-view response maps for radiometer detectors 13 and 29. These maps are useful to subjectively evaluate the spatial response, especially to reveal vignetting problems and locate sources of scatter. These maps are logarithmic plots of the relative spatial responsivity, with each contour representing a response of a factor of 2 below the preceding contour. Ten contours are shown in the figures, representing responses down to .001 of the peak. The map for detector 13, which is typical of the small radiometer detectors, shows that the major scatter areas included nearby detectors on the same substrate and regions

For all small detectors, the solid angles defined by the 0.5 contour were consistent with the design fields of view. More than half of their response to a spatially uniformly scene was from regions outside their 0.5-response contours. Using a 0.1-contour threshold, the solid angles were typically 5 times larger than the design solid angle, and scatter coefficients ranged from 30 to 50%, depending on detector.

The effective field-of-view solid angle of a sensor correlates its point-source response to its extended-source response. This correlation allows irradiance responsivity to be determined from radiance responsivity. The effective field-of-view solid angle is defined in terms of a hypothetical, spatially ideal sensor. This hypothetical sensor has the following characteristics: 1) The ideal sensor's response is zero at all spatial positions outside its field of view; 2) The ideal sensor's response to a point source at all spatial positions within its field of view is equal to the sensor's peak spatial response; and 3) The ideal sensor's response to an extended, spatially uniform source is equal to the actual sensor's response to the same spatially uniform source. The effective field-of-view solid angle of an actual sensor is equal to the field-of-view solid angle of this ideal sensor.

Effective field-of-view solid angles were computed for the IBSS radiometer detectors by:

$$\Omega_{eff} - \Delta X \Delta Y \sum\nolimits_{Total\ FP} Resp \qquad (8)$$

where Ω_{eff} = effective field-of-view solid angle in steradians, $\Delta X \Delta Y$ = incremental solid angle for each spatial response data point in steradians, and Resp = point-source responses. The effective fields of view were larger than design values for most detectors. This increase was mostly due to scatter.

The spatial response of a radiometer can also be evaluated in terms of its modulation transfer function (MTF), which describes its relative responsivity to different spatial frequencies. The MTF of a sensor can be computed using Fourier analysis of a point-source scan or a slit-source scan. The slit-source method shows the full MTF degradation due to scatter, while the point-source method is less affected by scatter, giving a more realistic MTF for point sources.

Calibration personnel computed a mean point-source scan for the radiometer detectors by averaging two or three spatial scans through each detector. The mean scans were then Fourier transformed and peak-normalized to give the MTFs. The slit-source MTFs were calculated in the same way as the point-source MTFs, except that all spatial response data were used to calculate the mean scans. This is equivalent to the scan of a long slit which covers the full height of the radiometer field of view. Figs. 12 and 13 present the MTF analysis for detector 13 in the X direction. A similar analysis was performed for each radiometer detector, in both the X and Y directions.
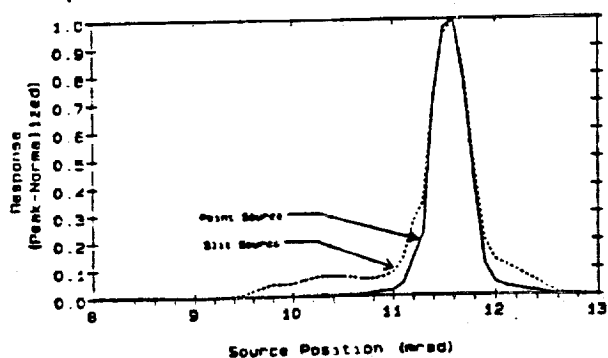

Fig. 12. Mean spatial scans for radiometer detector 13 in the X direction.
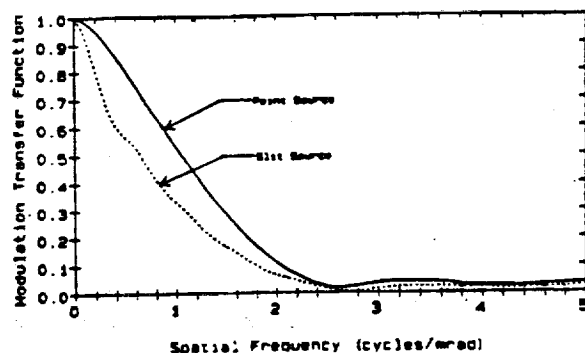
Fig. 13. MTFs for radiometer detector 13 in the X direction.

PRECEDING PAGE BLANK NOT FILMED

The sensor radiometric model includes the scan mirror position calibration, relating the sensor line of sight to scan mirror position reported by telemetry. The IBSS scan mirror position was calibrated by placing a collimated, 80-μrad source at fifteen different positions in object space, and collecting data with the IBSS mirror scanning. For each calibrator point-source position, the corresponding IBSS scan mirror position in counts was determined from the peak response of a chosen detector. These fifteen points were curve-fit to give a linear transfer function of scan mirror position in telemetry counts to sensor line of sight in mrad.

Temporal domain characterization

As with other sensors, the IBSS radiometer and spectrometer are frequency band-limited systems which cannot measure rapid scene modulations exactly. By understanding the sensor frequency response, however, experimenters may predict the effects of changing scenes on sensor response. Flux modulations result directly from time-varying sources, spatial scans of a spatially modulated scene for the radiometer, or spectral scans of a spectrally modulated scene for the spectrometer.

To measure the IBSS frequency response, calibration personnel illuminated the radiometer and spectrometer with radiation modulated by an external chopper at frequencies from 5 to 35 Hz for the radiometer and 10 to 100 Hz for the spectrometer (with the grating stopped). Fourier analysis of the resulting responses gave the energy in the chopper fundamental frequency. The response at each frequency was converted to decibels relative to the lowest chopper frequency measured. Fig. 14 shows the resulting relative frequency responses for the radiometer and spectrometer.
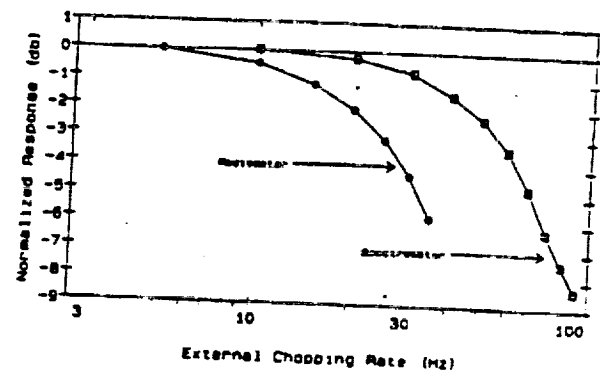

Fig. 14. Radiometer and spectrometer frequency response.

4. SUMMARY

This paper describes the methods used by SDL/USU to calibrate radiometric sensors. The calibrations of the IBSS infrared radiometer and spectrometer were given as specific examples using this calibration approach.

The calibration involved generating a specific calibration equation and radiometric model to describe the overall sensor responsivity with individual radiometric parameters. Calibration tests were then devised to characterize each radiometric parameter independent of the others. A cryogenic four-function calibration source was designed and fabricated to perform these tests. This source enabled calibration personnel to collect all data required for a full calibration in two 15-working day periods. This paper included terms from the IBSS calibration equation describing sensor dark offset, linearity, absolute responsivity, and measurement uncertainties. It also characterized the IBSS radiometric model in the spectral, spatial, and temporal responsivity domains.

5. ACKNOWLEDGMENTS

6. REFERENCES

1. G. Lange, E. Weichs, U. Schmidt, D. Sodeikat, "Spectrometer/Radiometer for Measurement of IR Signatures From Space," _Proceedings of SPIE - The International Society of Optical Engineering_, vol. 940, 1990.

2. C.L. Wyatt, _Radiometric Calibration: Theory and Methods_, Academic Press, New York, 1978.

3. C.L. Wyatt, L. Jacobsen, A. Steed, "Portable Compact Multifunction IR Calibrator," _Proceedings of SPIE - The International Society of Optical Engineering_, vol 940, pp. 63-72, 1988.

4. L. Jacobsen and S. Sargent, "IBSS IR Sensor Calibration Final Report," Space Dynamics Laboratory/Utah State University No. SDL/89-119, January 1990.

THIS PAGE LEFT BLANK INTENTIONALLY